Journal of Bacteriology

Analysis of SOS-Induced Spontaneous Prophage Induction in Corynebacterium glutamicum at the Single-Cell Level

Arun M. Nanda, Antonia Heyer, Christina Krämer, Alexander Grünberger, Dietrich Kohlheyer and Julia Frunzke

J. Bacteriol. **2014, 196(1):180. DOI: 10.1128/JB.01018-13.**
Published Ahead of Print 25 October 2013.

JB
Journals.ASM.org

Analysis of SOS-Induced Spontaneous Prophage Induction in *Corynebacterium glutamicum* at the Single-Cell Level

Arun M. Nanda, Antonia Heyer, Christina Krämer, Alexander Grünberger, Dietrich Kohlheyer, Julia Frunzke

Institut für Bio- und Geowissenschaften, IBG-1: Biotechnologie, Forschungszentrum Jülich, Jülich, Germany

The genome of the Gram-positive soil bacterium *Corynebacterium glutamicum* ATCC 13032 contains three integrated prophage elements (CGP1 to -3). Recently, it was shown that the large lysogenic prophage CGP3 (~187 kbp) is excised spontaneously in a small number of cells. In this study, we provide evidence that a spontaneously induced SOS response is partly responsible for the observed spontaneous CGP3 induction. Whereas previous studies focused mainly on the induction of prophages at the population level, we analyzed the spontaneous CGP3 induction at the single-cell level using promoters of phage genes (P_{int2} and P_{lysin}) fused to reporter genes encoding fluorescent proteins. Flow-cytometric analysis revealed a spontaneous CGP3 activity in about 0.01 to 0.08% of the cells grown in standard minimal medium, which displayed a significantly reduced viability. A P_{recA}-*eyfp* promoter fusion revealed that a small fraction of *C. glutamicum* cells (~0.2%) exhibited a spontaneous induction of the SOS response. Correlation of P_{recA} to the activity of downstream SOS genes (P_{divS} and P_{recN}) confirmed a bona fide induction of this stress response rather than stochastic gene expression. Interestingly, the reporter output of P_{recA} and CGP3 promoter fusions displayed a positive correlation at the single-cell level ($\rho = 0.44$ to 0.77). Furthermore, analysis of the P_{recA}-*eyfp*/P_{int2}-*e2-crimson* strain during growth revealed the highest percentage of spontaneous P_{recA} and P_{int2} activity in the early exponential phase, when fast replication occurs. Based on these studies, we postulate that spontaneously occurring DNA damage induces the SOS response, which in turn triggers the induction of lysogenic prophages.

Genome sequencing projects have revealed a large amount of prophage DNA in bacterial genomes. Although not all prophage DNA accounts for functional prophages, because it includes degenerated phage remnants, this DNA can have a marked impact on bacterial physiology (1). The biotechnological platform organism *Corynebacterium glutamicum* is a Gram-positive, biotin-auxotroph soil bacterium that is used for the industrial production of more than four million tons of L-glutamate and L-lysine per year (2, 3). As revealed by whole-genome sequencing, *C. glutamicum* ATCC 13032 possesses three prophages that are integrated into its genome (CGP1 to -3), of which CGP1 and CGP2 are probably degenerated phage remnants (4–6). Previous studies showed that the large prophage CGP3 (187 kb) retains the ability to be excised from the genome and exist as a circular DNA molecule. Interestingly, a small number of wild-type cells showed a much higher copy number of circular phage DNA per cell than the average of the population (5).

Recent studies in *Shewanella oneidensis* (7) and *Streptococcus pneumoniae* (8) have provided evidence that sacrificing a small number of cells by spontaneous prophage-induced lysis is beneficial to the remainder of the population. For these species, genomic DNA released into the extracellular space following cell lysis supports biofilm formation and maintenance (9, 10). Although these results shed new light on the spontaneous induction of prophages, the mechanisms governing this general microbiological phenomenon are poorly understood to date.

The best-studied model for prophage-host interactions is the *Escherichia coli* λ phage model. As far back as the 1950s, spontaneous induction of lysogenic phage λ was observed in *E. coli* cultures (11). Remarkably, a decrease in spontaneously induced prophages was shown in recombination-deficient *E. coli* strains (12). It remains unknown, however, whether these events are (i) random events caused by promoter noise or by the stochastic distribution of key regulatory components or (ii) the result of specific induction by intrinsic and/or extrinsic factors. The lysogenic state of phage λ is controlled by cI, the central repressor of phage genes (13). When the integrity of the genome is compromised (as indicated by lesions in the DNA), the protein RecA polymerizes along single-stranded DNA (ssDNA). This nucleoprotein filament of ssDNA and activated RecA* protein catalyzes the autocatalytic cleavage of the repressor LexA, which leads to the derepression of more than 40 SOS genes (SOS response) (14). The life cycle of lambdoid phages is linked to this regulatory pathway. The central repressor cI mimics the autocatalytic center of LexA and thus becomes cleaved upon the induction of the SOS response. Its binding to repressor sites within the prophage is alleviated, leading to an expression of genes responsible for the excision of phage DNA, virion assembly, and release of the infectious phage particles into the extracellular space (13).

In this study, we address the question of whether the spontaneous induction of the lysogenic prophage CGP3 in single *C. glutamicum* cells is linked to the spontaneous activation of the SOS response. The promoters of genes of the SOS pathway and those encoded by CGP3 were fused to the fluorescent reporter genes *eyfp* and *e2-crimson* to analyze the activity of the respective promoters under standard cultivation conditions. Single-cell analysis was performed using flow cytometry and an in-house developed polydimethylsiloxane (PDMS) microfluidic chip setup (15, 16) suit-

Received 27 August 2013 **Accepted** 21 October 2013
Published ahead of print 25 October 2013
Address correspondence to Julia Frunzke, j.frunzke@fz-juelich.de.
Supplemental material for this article may be found at http://dx.doi.org/10.1128/JB.01018-13.

doi:10.1128/JB.01018-13

TABLE 1 Bacterial strains and plasmids used in this study

Strain or plasmid	Characteristics	Source or reference
Strains		
E. coli DH5α	*supE44* Δ*lacU169* (ϕ80*lacZ*DM15) *hsdR17 recA1 endA1 gyrA96 thi-1 relA1*	Invitrogen
C. glutamicum		
ATCC 13032	Biotin-auxotrophic wild type	36
ATCC 13032Δ*lexA*	In-frame deletion of the gene *lexA* (cg2114)	22
ATCC 13032::P_{recA}-*eyfp*	Integration of P_{recA}-*eyfp* into the intergenic region between cg1121 and cg1122	This study
Plasmids		
pJC1	Kan^r, Amp^r; *C. glutamicum* shuttle vector	38
pEKEx2-P_{tac}-*eyfp*	Kan^r; pEKEx2 containing *eyfp* with pET16 RBS, under the control of P_{tac}	23
pAN6-*e2-crimson*	Kan^r; pAN6 derivative for expression of E2-Crimson under the control of the P_{tac} promoter	6
pK19*mobsacB*	Kan^r, $oriV_{E. coli}$ *sacB lacZ*α	37
pK18*mobsacB*-cg1121/1122	Kan^r, $oriV_{E. coli}$ *sacB*	6
pK18*mobsacB*-cg1121/1122-P_{recA}-*eyfp*	pJC1 derivative containing the promoter of *recA* (260 bp) fused to *eyfp*; the insert includes the promoter of *recA* and an additional ribosome binding site (pET16) in front of *eyfp*	This study
pJC1-P_{divS}-*e2-crimson*	pJC1 derivative containing the promoter of *divS* (411 bp) fused to *e2-crimson*; the insert includes the promoter of *divS*, 30 bp of the coding sequence, a stop codon, and an additional ribosome binding site (pET16) in front of *e2-crimson*	This study
pJC1-P_{recN}-*e2-crimson*	pJC1 derivative containing the promoter of *recN* (207 bp) fused to *e2-crimson*; the insert includes the promoter of *recN*, 30 bp of the coding sequence, a stop codon, and an additional ribosome binding site (pET16) in front of *e2-crimson*	This study
pJC1-P_{int2}-*e2-crimson*	pJC1 derivative containing the promoter of *int2* (250 bp) fused to *e2-crimson*; the insert includes the promoter of *int2*, 30 bp of the coding sequence, a stop codon, and an additional ribosome binding site (pET16) in front of *e2-crimson*	This study
pJC1-P_{lysin}-*e2-crimson*	pJC1 derivative containing the promoter of *lysin* (250 bp) fused to *e2-crimson*; the insert includes the promoter of *lysin*, 30 bp of the coding sequence, a stop codon, and an additional ribosome binding site (pET16) in front of *e2-crimson*	This study
pJC1-P_{cg2067}-*e2-crimson*	pJC1 derivative containing the promoter of cg2067 (250 bp) fused to *e2-crimson*; the insert includes the promoter of cg2067, 30 bp of the coding sequence, a stop codon, and an additional ribosome binding site (pET16) in front of *e2-crimson*	This study

able for observing rare cellular events of interest. We observed a positive correlation between the spontaneous activation of the SOS response and the spontaneous induction of the prophage CGP3, and we postulate a bona fide activation of the SOS response as a prominent trigger leading to prophage excision.

MATERIALS AND METHODS

Bacterial strains, media, and growth conditions. The bacterial strains used in this study are listed in Table 1. *C. glutamicum* ATCC 13032 was used as the wild-type strain; all strains were cultivated at 30°C. For growth experiments, a glycerin stock culture was streaked onto BHI (brain heart infusion; Difco, BD, Heidelberg, Germany) agar plates. Single colonies were used to inoculate 5 ml liquid BHI medium. After cultivation for 8 h, the preculture was used to inoculate 25 ml CGXII minimal medium (1:50) containing 4% glucose (wt/vol) as the carbon source (17). After growth overnight, fresh CGXII medium was inoculated to an optical density at 600 nm (OD_{600}) of 1 in 25 ml. For microtiter-scale cultivations, the Biolector microbioreactor system (m2p-labs, Heinsberg, Germany) was utilized (18) using an established protocol for *C. glutamicum* cultivation (16). *Escherichia coli* was cultivated in LB (lysogeny broth) medium and on LB agar plates at 37°C. If required, kanamycin was added to the cultivation medium at a concentration of 25 μg/ml for *C. glutamicum* and 50 μg/ml for *E. coli*. For induction of the SOS response, mitomycin C (Sigma-Aldrich, Seelze, Germany) was added at the appropriate concentrations at an OD_{600} of 4.

Cloning techniques. For PCR amplification of DNA used for cloning, KOD HotStart polymerase (Merck Millipore, Darmstadt, Germany) was used. DreamTaq (Fisher Scientific, Schwerte, Germany) was utilized for PCR verification of ligation reactions. Heat shock transformation of *E. coli* was performed as described previously (19). Transformation of *C. glutamicum* was performed by electroporation as described previously (20). Isolation and purification of plasmids from *E. coli* cultures was performed using plasmid isolation and purification kits from Qiagen (Qiagen, Hilden, Germany) and Thermo Scientific (Fisher Scientific, Schwerte, Germany) miniprep kits. Chromosomal DNA of *C. glutamicum* was isolated as described previously (21). DNA sequencing and oligonucleotide synthesis were performed by Eurofins MWG Operon (Ebersberg, Germany). Plasmids and oligonucleotides used in this work are listed in Table 1 and Table 2, respectively. The in-frame deletion mutant of *lexA* in the wild-type strain ATCC 13032 was constructed as described by Jochmann et al. (22).

Construction of promoter fusions. For construction of the promoter fusions of P_{int2}, P_{lysin}, and P_{cg2067}, 250 bp upstream of the coding sequence with an additional 10 codons and the 16-bp ribosomal binding site of pET16 were amplified using the oligonucleotide pairs int2-fwd/int2-rev, lysin-fwd/lysin-rev, and cg2067-fwd/cg2067-rev, respectively. The promoter sequences were ligated into the vector pJC1-crimson-term by restriction with BamHI and NdeI.

For construction of the *recA* promoter fusion, 260 bp upstream of the coding sequence were amplified from genomic *C. glutamicum* DNA followed by the 16-bp ribosomal binding site of pET16 using oligonucleotides PrecA_pK18_fwd and PrecA_YFP_rev. *eyfp* was amplified with oligonucleotides YFP_fwd and YFP_pK18_rev using the plasmid pEKEx2-P_{tac}-*eyfp* (23) as the template. The promoter fusion was generated by overlap extension PCR using oligonucleotides PrecA_pK18_fwd and PrecA_YFP_rev. XhoI and MfeI restriction sites were used to ligate

TABLE 2 Oligonucleotides used in this study

Oligonucleotide	Sequence (5′–3′)[a]	Restriction site
cg2114_del_1	TCCCCCGGGGATCTAGGATCCACATGGAAGCGAACAGAG	SmaI
cg2114_del_2	TGAAGTCCTGCAGCATCA	
cg2114_del_3	TGATGCTGCAGGACTTCATGTTGGCGAGTCCATGAG	
cg2114_del_4	GCTCTAGAGATCTACTGCAGCGCCACGATATGTGAGAA	XbaI
PrecA_pK18_fwd	GGAATTCAATTGTTCGCATGAAAATTCGAATT	MfeI
PrecA_YFP_rev	GCTCACCATATGTATATCTCCTTTTTTAATTCCTCTTAGTTTTATTGA	
YFP_fwd	AAGGAGATATACATATGGTGAGCAAGGGCGA	
YFP_pK18_rev	GGAATTCTCGAGTTATCTAGACTTGTACAGCTCGTCCAT	XhoI
divS_fwd	CTAGCTAGCTAGCGTTGGGCAAGGTCTTAACT	NheI
divS_rev	ATGATATCTCCTTCTTAAAGTTTAATCTAGCTCTTTACCCGCATAAAC	
crimson_fwd	TAAACTTTAAGAAGGAGATATCATATGGATAGCAC	
crimson_rev	CTAGCTAGCTAGCAAAAGAGTTTGTAGAAACGC	NheI
int2_fwd	CGCGGATCCCGGGCGAGAGGGTGAGCGAT	BamHI
int2_rev	CGCCATATGATATCTCCTTCTTAAAGTTCAGAAGCGTGCCCTGTACCTCTCCGA	NdeI
lysin_fwd	CGCGGATCCCCTTCTTTGAGGCTTGATGCCT	BamHI
lysin_rev	CGCCATATGATATCTCCTTCTTAAAGTTCAATTTTTCGGCATTGCGCCTTTAAT	NdeI
cg2067_fwd	CGCGGATCCGAAGCTTTTGAGTCTGTTACTGG	BamHI
cg2067_rev	CGCCATATGATATCTCCTTCTTAAAGTTCACGACCACATCTCCAACGCGCTAAA	NdeI

[a] Restriction sites are underlined.

the amplicon into the shuttle vector pK18mobsacB_cg1121/22. Promoter fusions of *divS* and *recN* were amplified with the oligonucleotides divS_fwd and divS_rev and the oligonucleotides recN_fwd and recN_rev, respectively, using genomic DNA as the template. Additionally, the first 10 codons were amplified along with a stop codon. The coding sequence of the fluorescent protein E2-Crimson (24) was amplified from the plasmid pAN6-*e2-crimson* with the oligonucleotides crimson_fwd and crimson_rev. Both amplicons were combined by overlap extension PCR. The restriction site NheI was used for ligation into the medium-copy-number vector pJC1.

The P_{ptsG}-*e2-crimson* promoter fusion was constructed according to Hentschel et al. (23) by amplifying 725 bp upstream of the *ptsG* start codon with oligonucleotides PptsG_fwd and PptsG_rev, introducing BamHI and NdeI restriction sites. The PCR fragment was ligated into pJC1-e2-crimson-term after treatment of both with BamHI and NdeI restriction enzymes.

Fluorescence microscopy. For phase contrast and fluorescence microscopy, samples were analyzed on 1 to 2% agar pads, which were placed on microscope slides and covered by a coverslip. Images were taken on a Zeiss Axioplan 2 imaging microscope equipped with an AxioCam MRm camera and a Plan-Apochromat ×100 magnification, 1.4 numerical-aperture oil differential interference contrast (DIC) objective. Filter sets 46HE and 63HE were used for imaging enhanced yellow fluorescent protein (eYFP) and E2-Crimson fluorescence, respectively. Digital images were acquired and analyzed with the AxioVision 4.6 software (Zeiss, Göttingen, Germany).

Flow cytometry. Flow-cytometric measurements and sorting were performed on a FACSAria II (Becton, Dickinson, San Jose, CA) flow cytometer with 488-nm excitation by a blue solid-state laser and 633-nm excitation by a red solid-state laser. Forward-scatter characteristics (FSC) and side-scatter characteristics (SSC) were detected as small- and large-angle scatters of the 488-nm laser, respectively. eYFP fluorescence was detected using a 502-nm long-pass and a 530/30-nm band pass filter set. E2-Crimson fluorescence was detected using a 660/20-nm band pass filter set. Cells were analyzed at a threshold rate of 3,000 to 8,000 events/s and sorted onto BHI agar plates at a threshold rate of 3,000 to 4,000 events/s. Data were analyzed using FlowJo V7.6.5 (Tree Star, Inc., Ashland, OR).

Statistical analysis. Nonparametric tests for the analysis of correlation were performed with GraphPad Prism 6 (GraphPad Software, Inc., La Jolla, CA). Spearman's rank correlation coefficient (the Pearson correlation coefficient of the ranked variables) was used. A perfect (inverse) correlation takes on ρ values of (−)1; totally independent variables take on ρ values of 0.

Microfluidic cultivation. *C. glutamicum* was cultivated in in-house-developed microfluidic cultivation chambers (0.9 μm by 60 μm by 60 μm) arranged in parallel between 10-fold-deeper supply channels. For details on our microfluidic chip setup, see references 15 and 25.

During the experiment, CGXII minimal medium was infused continuously at 300 nl min^{-1} using a high-precision syringe pump (neMESYS; Cetoni GmbH, Korbussen, Germany) with attached disposable syringes (Omnifix-F Tuberculin, 1 ml; B. Braun Melsungen AG, Melsungen, Germany) to maintain constant environmental conditions. Cell growth and eYFP fluorescence were observed at 10-min intervals by time-lapse imaging with a fully motorized inverted Nikon Eclipse Ti microscope (Nikon GmbH, Düsseldorf, Germany). Chip cultivation was performed at 30°C using a microscope incubator system (PeCon GmbH, Erbach, Germany). The microscope was equipped with a focus assistant (Nikon PFS) to compensate for thermal drift during long-term microscopy, with a Plan Apo λ 100× oil Ph3 DM objective (Nikon GmbH, Düsseldorf, Germany) and a high-speed charge-coupled device (CCD) camera (Andor Clara DR-3041; Andor Technology Plc., Belfast, United Kingdom). An optical filter system (YFPHQ filter system [excitation, 490 to 550 nm; dichroic mirror, 510 nm; absorption filter, 520 to 560 nm]; AHF Analysentechnik AG, Tübingen, Germany) and a mercury light source (Intensilight; Nikon GmbH, Düsseldorf, Germany) were installed for fluorescence microscopy.

RESULTS

The prophage CGP3 is spontaneously induced in single cells. In recent studies we observed a spontaneous excision of the prophage CGP3 in a small number of *C. glutamicum* cells cultivated in shake flasks with CGXII minimal medium (5). Transcriptome analysis revealed an upregulation of CGP3 genes (cg1890 to cg2071) upon induction of the SOS response by addition of the DNA-cross-linking antibiotic mitomycin C (A. Heyer and J. Frunzke, personal communication). In an effort to create appropriate tools to monitor prophage activity, we consulted reports on previous microarray experiments to determine which genes are suitable candidates. We constructed plasmid-based promoter fusions of the CGP3 genes cg2071 (integrase, *int2*), cg1974 (putative lysin), and cg2067 (hypothetical protein) to the coding sequence of the fluorescent protein E2-Crimson. To test their function, wild-type *C. glutamicum* ATCC 13032 cells were transformed with the

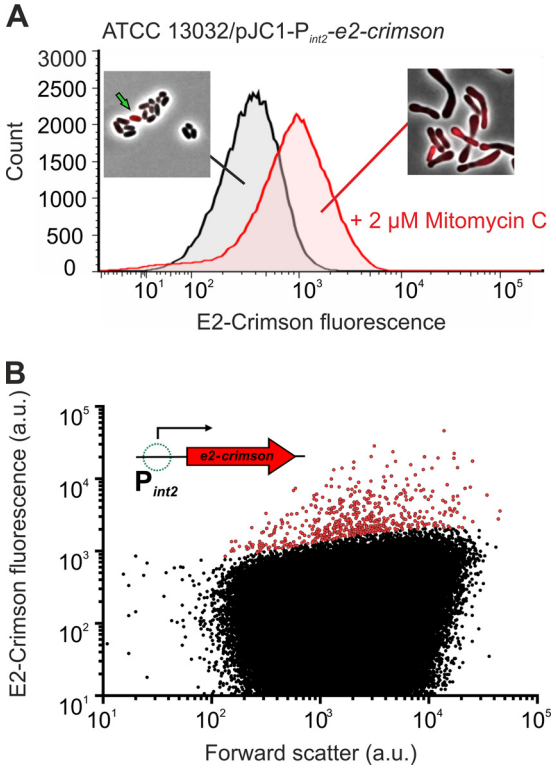

FIG 1 Utilization of prophage promoter fusions for monitoring spontaneous CGP3 induction. (A) Histogram of eYFP fluorescence of *C. glutamicum*/pJC1-P$_{int2}$-*e2-crimson* with 2 μM mitomycin C (red line) and without mitomycin C (gray line) with additional fluorescence microscopy images showing the spontaneous and induced activity of P$_{int2}$. The insets show uninduced and induced cells carrying the plasmid pJC1-P$_{int2}$-*e2-crimson*. The green arrow indicates spontaneous induction of P$_{int2}$ occurring under standard cultivation conditions. (B) Scatter plot of the strain *C. glutamicum*/pJC1-P$_{int2}$-*e2-crimson*. A total of 100,000 cells were analyzed for their size characteristics (forward scatter) and their fluorescent properties. Even under noninducing conditions, a small fraction of cells exhibited an increased reporter signal (red dots) in comparison to the bulk of the population (black dots). Cells were cultivated in CGXII medium plus 4% glucose and analyzed at an OD$_{600}$ of 4.

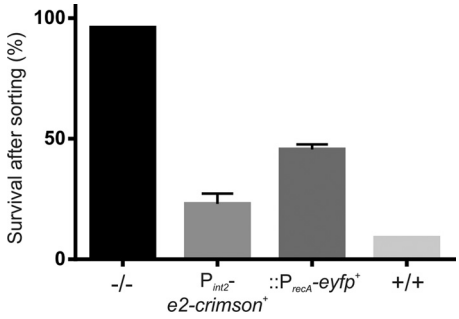

FIG 2 Viability assay of *C. glutamicum* cells which exhibit an induction of CGP3 and/or of the SOS response. Single cells were sorted onto agar plates, and the percent survival was determined as the fraction of cells able to form colonies. Nonfluorescent cells (−/−), cells with either a positive P$_{recA}$-*eyfp* or a positive P$_{int2}$-*e2-crimson* signal (+), and cells with both signals (+/+) were sorted onto separate agar plates. Colony growth was analyzed after 24 h.

promoter fusion constructs and treated with 2 μM mitomycin C to induce DNA lesions and subsequently trigger the SOS response. Samples were analyzed by flow cytometry and fluorescence microscopy (shown for P$_{int2}$) (Fig. 1A). The treated samples exhibited a highly induced P$_{int2}$ activity and morphological changes. The untreated cultures showed no significant P$_{int2}$ activity, yet, in agreement with earlier studies, P$_{int2}$ was highly induced in a small number of cells. Flow-cytometric analysis of untreated cultures revealed that a fraction of 0.01 to 0.08% of the cells exhibited a 5- to 160-fold higher P$_{int2}$ activity than the bulk of the population (Fig. 1B). Single cells with a high fluorescent signal (phage$^+$) and cells showing background fluorescence (phage$^-$) were sorted onto BHI agar plates, and their survival was assessed after incubation for 24 h. As expected, the survival rate of phage$^+$ cells was significantly below that of phage$^-$ cells (survival rates of 23% and 96%, respectively) (Fig. 2). Thus, cells showing an increased P$_{int2}$ activity were significantly impaired in their ability to resume growth on plates, which is likely caused by prophage excision and subsequent cell lysis.

Spontaneous P$_{recA}$ induction in single cells. Since the host SOS response is a prominent trigger of lysogenic phages, we constructed a promoter fusion of the *recA* promoter to *eyfp* and integrated it into the genome of *C. glutamicum* ATCC 13032 at the intergenic region of cg1121 and cg1122 to test for a spontaneous SOS induction. As proof of principle, the P$_{recA}$-*eyfp* strain was cultivated in microtiter scale and the SOS response was induced by addition of mitomycin C in increasing concentrations. A strain with a truncation of *lexA*, the repressor of SOS genes, served as a reference strain which exhibits a maximally induced SOS response (Fig. 3A, black bar). At low concentrations (15 nM and 100 nM) of mitomycin C and in the Δ*lexA* strain, P$_{recA}$ activity showed a bimodal distribution, with the majority of cells showing a slight increase in reporter signal and a smaller fraction of cells shifted toward an even higher signal. This bimodal state was not observed at higher concentrations (500 nM and 1,000 nM mitomycin C) (Fig. 3B). We subjected cells with the integrated P$_{recA}$-*eyfp* promoter fusion to flow-cytometric analysis to get more detailed insight into single-cell dynamics of the SOS response in *C. glutamicum* populations. Under standard cultivation conditions, we observed a spontaneous activity, analogous to the activities of CGP3 promoters (Fig. 3C). About 0.07 to 0.2% of cells showed a 12- to 18-fold increased reporter signal (SOS$^+$ cells). These SOS$^+$ cells had a reduced survival rate (recovery rate of 46% after sorting on BHI agar plates) (Fig. 2). It was tempting to hypothesize that these rare events may act as a bet-hedging strategy to ensure an increased fitness under changing environmental conditions. We sorted SOS$^+$ cells on agar plates with different DNA damaging conditions yet saw no increased fitness under the tested conditions (data not shown).

Spontaneous P$_{recA}$ activity reflects a bona fide SOS response. Next we tested whether spontaneous P$_{recA}$ activity and reduced viability were indicative of a bona fide SOS response caused by potentially lethal DNA damage. The reporter strain harboring the integrated promoter fusion P$_{recA}$-*eyfp* was transformed with plasmids carrying promoter fusions of the two SOS-responsive genes *divS* and *recN*, respectively, fused to the autofluorescent reporter gene *e2-crimson*. Both genes were previously shown to be upregulated in the deletion mutant Δ*lexA* (22) or after induction with mitomycin C. Analysis of the dual reporter strain (P$_{recA}$-*eyfp* integrated into the genome, P$_{int2}$-*e2-crimson* plasmid-borne) by fluorescence microscopy and flow cytometry revealed a correlation of the P$_{recA}$ signal to P$_{divS}$ as well as P$_{recN}$ signals. After gating of SOS$^+$

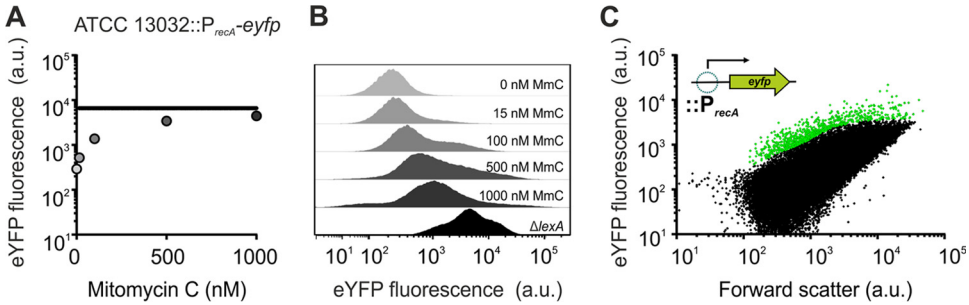

FIG 3 P$_{recA}$ promoter fusion for the analysis of SOS induction in single cells. (A) Dose response plotted as mean eYFP fluorescence at increasing mitomycin C (MmC) concentrations. (B) Offset histogram of *C. glutamicum*::P$_{recA}$-*eyfp* cells subjected to increasing concentrations of mitomycin C. *C. glutamicum* Δ*lexA* was used as a reference strain which exhibits maximal induction of the SOS response. (C) Scatter plot of the strain *C. glutamicum*::P$_{recA}$-*eyfp* cultivated under nonstressful conditions. A total of 100,000 cells were analyzed for their size characteristics (forward scatter) and their fluorescent properties. A small fraction of cells exhibits an increased reporter signal (green dots) in comparison to the bulk of the population (black dots). Cells were cultivated in CGXII medium plus 4% glucose in the Biolector system until the stationary phase.

cells, the signals of both reporters were correlated in single cells by using Spearman's rank correlation coefficient (Fig. 4). Both promoter fusions showed a high correlation (P$_{divS}$, $\rho = 0.78$, $P < 0.0001$, $n = 165$; P$_{recN}$, $\rho = 0.85$, $P < 0.0001$, $n = 131$) at the single-cell level. The control promoter fusion P$_{ptsG}$-*e2-crimson* was constructed and introduced into the P$_{recA}$-*eyfp* strain to exclude high correlation values due to factors other than sharing the same regulation. SOS$^+$ cells were gated and their P$_{recA}$ signal correlated to the P$_{ptsG}$ reporter signal. Both signals displayed a low correlation ($\rho = 0.36$, $P < 0.0001$, $n = 248$). Thus, the strong correlation of P$_{recA}$ to P$_{divS}$ and P$_{recN}$ activities confirmed that a spontaneous P$_{recA}$ activity in single cells leads to a bona fide induction of the downstream SOS cascade.

Time-lapse analysis of P$_{recA}$ activation dynamics. SOS$^+$ cells did not display a uniform fate, with some cells being able to survive on agar plates whereas others were not viable. For a time-resolved analysis of the SOS induction in single cells, we cultivated the P$_{recA}$-*eyfp* strain in an in-house-developed PDMS microfluidic system enabling spatiotemporal analysis of growing microcolonies by automated time-lapse microscopy. Single cells were seeded into the microfluidic cultivation chambers and cultivated for several generations in standard CGXII minimal medium under nonstressful conditions; images were acquired every 10 min. Again, we observed different fates of SOS$^+$ cells (see Movies S1 to S3 in the supplemental material). Some cells showed a high and continuous reporter signal together with an elongated cell morphology and growth inhibition caused by an activated SOS response (Fig. 5; also, see Movies S1 to S3 in the supplemental material). These bacteria represent cells which undergo severe DNA damage, triggering the SOS response. However, other cells merely showed a pulse of the reporter along with an unaltered growth and cell morphology (Fig. 5; also, see Movies S1 and S2 in the supplemental material). This output either represents activity due to the stochastic binding of repressor molecules or might be triggered by DNA damage which is repaired before a full-blown SOS response is initiated. Furthermore, we observed an additional cell fate which consisted of high induction of the reporter coupled with an elongated cell morphology, growth inhibition, and cell branching (see Movie S3 in the supplemental material). This is analogous to *C. glutamicum* cells which continuously overexpress *divS* under the control of the promoter P$_{aceA}$ (26), indicating a high concentration of DivS in these cells.

Correlating prophage activity to an induced SOS response in single cells. Having established promoter fusions for the analysis of spontaneous CGP3 induction and SOS response, we combined promoter fusions of *recA* and of the prophage genes to correlate

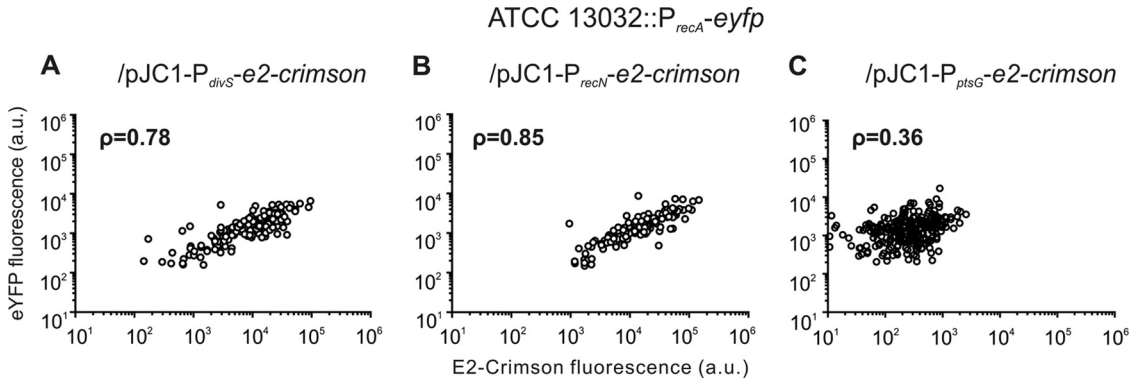

FIG 4 Correlation of P$_{recA}$ activity to the activity of promoters of downstream SOS genes. Scatter plots of *C. glutamicum*::P$_{recA}$-*eyfp*/pJC1-P$_{divS}$-*e2-crimson* (A), *C. glutamicum* P$_{recA}$-*eyfp*/pJC1-P$_{recN}$-*e2-crimson* (B), and *C. glutamicum* P$_{recA}$-*eyfp*/pJC1-P$_{ptsG}$-*e2-crimson* (C) are shown; *C. glutamicum* P$_{recA}$-*eyfp*/pJC1-P$_{ptsG}$-*e2-crimson* served as a control, reflecting the correlation of *recA* expression and an SOS-independent promoter. Cells with high eYFP fluorescence (spontaneous P$_{recA}$-*eyfp* cells) were gated and are displayed in the dot plot of eYFP fluorescence versus E2-Crimson fluorescence. Spearman's rank correlation coefficient (ρ) was calculated using GraphPad Prism 6. Cells were cultivated in CGXII medium plus 4% glucose and analyzed at an OD$_{600}$ of 4.

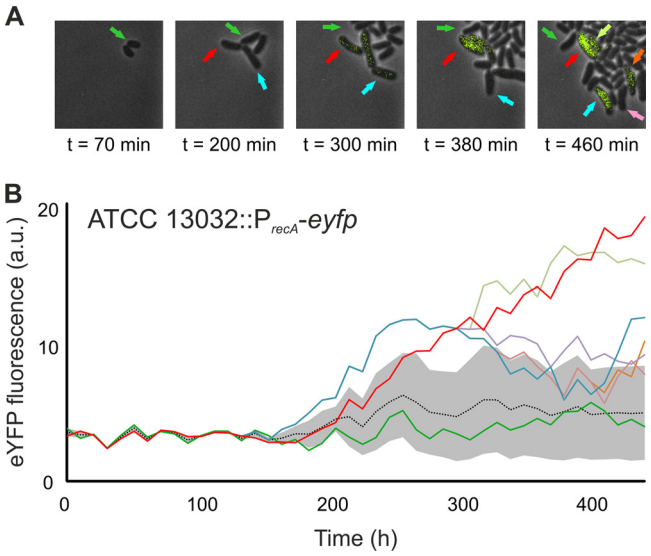

FIG 5 Fluorescence traces of P_{recA} activity in single cells observed by live cell imaging. Cells harboring the integrated P_{recA}-*eyfp* promoter fusion were seeded into the microfluidic chip and cultivated for 24 h; a representative microcolony is shown. (A) Microscopic images of microcolony during cultivation. Single cells were analyzed for their fluorescent output and assigned a unique cell ID (colored arrow). (B) Course of fluorescence for single cells (colored lines) as well as for the entire microcolony (mean value, plotted as a dotted line; standard deviations are shown as a gray area). Single cells either showed no fluorescence (green trace), showed a high induction of P_{recA} (red and light green trace), displayed a pulsing behavior with no further promoter activity (violet and pink traces), or displayed a pulsing behavior followed by a high reporter signal (cyan and orange traces).

them at the single-cell level. To this end, the P_{recA}-*eyfp* strain was transformed with the P_{int2}, P_{lysin}, and P_{cg2067} promoter fusions to *e2-crimson*. Analysis by flow cytometry again showed the occurrence of spontaneously activated cells for both types of promoter fusions. Fluorescence microscopy revealed that not all cells showed an activation of the prophage promoters when P_{recA} was active (Fig. 6). To measure the interdependence of both signals, the Spearman rank correlation coefficient was calculated for both. The highest correlation to SOS^+ cells was observed for P_{cg2067} and P_{int2} (P_{cg2067}, $\rho = 0.77$, $P < 0.0001$, $n = 687$; P_{int2}, $\rho = 0.57$, $P < 0.0001$, $n = 828$) (Fig. 6). P_{lysin} showed the lowest correlation ($\rho = 0.44$, $P < 0.0001$, $n = 790$) under the tested conditions. Even though the correlation coefficient is not able to reveal a causal link between two processes, it did show a high correlation of the promoters of *recA* and the prophage genes. Reciprocal analysis of $phage^+$ cells was performed as well and gave nearly identical values (P_{cg2067}, $\rho = 0.72$, $P < 0.0001$, $n = 119$; P_{int2}, $\rho = 0.58$, $P < 0.0001$, $n = 565$; P_{lysin}, $\rho = 0.45$, $P < 0.0001$, $n = 759$) (data not shown). This correlation suggests a link between spontaneously induced SOS response and spontaneous activity of CGP3 in single cells. Nevertheless, correlation was lower than that between P_{recA} and P_{divS}/P_{recN}, indicating that others factors besides the SOS response might influence the activity of the prophage promoters.

Impact of growth phase on spontaneous SOS and prophage activity. The P_{recA}-*eyfp*/pJC1-P_{int2}-*e2-crimson* strain was cultivated in shake flasks, and samples were analyzed until the cells reached stationary growth phase (Fig. 7A) to eliminate the rigidity of measurements at single time points and better assess the characteristics of the reporters during growth. The P_{recA} signal showed maximal intensity at the transition to and during the early phase of exponential growth. Activity of P_{int2} showed the same behavior. We expected this parallel activation of both promoters, if the SOS response and prophage induction are somehow linked. The number of spontaneously activated cells was measured for all time points as well (Fig. 7B). Whereas the peaks of both reporters' fluorescent output behaved similarly, the maximal number of spontaneously activated $phage^+$ and SOS^+ cells showed a temporal disparity. The increase of SOS^+ cells was observed 2 h before the relative amount of $phage^+$ cells increased.

DISCUSSION

The present study on the induction of lysogenic prophages was performed on a population-wide scale. It was shown that the induction of lambdoid phages is typically linked to the host's SOS response. The underlying bistable switch (13), simplified by the action of the repressor of phage genes cI, is turned toward lytic growth when the host's SOS response becomes activated. Spontaneous induction of prophages had been observed as far back as the 1950s (11), yet studies since then have not explored this phenomenon in more detail at the single-cell level. Due to the general link between the SOS response and prophage induction, it was tempting to speculate that the cause of spontaneous prophage induction lies in a spontaneously induced SOS response. The data shown in this study suggest that a small fraction of *C. glutamicum* cells grown under standard conditions spontaneously induced expression of prophage genes and that this activation is caused in part by the spontaneous activity of the SOS response in single cells.

During the cultivation of wild-type cells under standard cultivation conditions, we observed single cells that induced the SOS response spontaneously. As the occurrence of spontaneous DNA breakage has previously been reported in studies on *E. coli* (27), we tested this in *C. glutamicum*. In the *E. coli* studies, use of the SOS-inducible promoter of the cell division inhibitor gene *sulA* fused to *gfp* revealed a spontaneous SOS response in about 0.9% of cells. The rate of spontaneous SOS induction that we measured with P_{recA}-*eyfp* lies at about 0.2%. When other LexA-regulated promoters of *C. glutamicum*, such as P_{divS}, P_{recN}, and P_{cglIM}, were used, the fraction of cells exhibiting a spontaneous SOS response lay between 0.1 and 0.5% (data not shown). Considering that further studies in *E. coli* using promoter fusions of *lexA*, *recA*, and *umuDC* showed spontaneous promoter activity in 0.09 to 3.1% of cells (28), our findings are consistent with those reported previously.

We assumed the SOS^+ cells to be impaired in their survival due to potentially lethal DNA damage. The survival rate of SOS^+ cells lay at 46%. Our microfluidic studies showed that an induction of the SOS response leads to the arrest of cell growth in some cells, probably caused by irreparable DNA damage, whereas other cells are able to resume growth after they exhibit P_{recA} activity. This activity in turn did not necessarily lead to a full-blown SOS response, as some cells showed the SOS phenotype; others, however, were either unaffected in their growth with a mere pulse of P_{recA} activity or were inhibited in their growth but able to recover from the SOS-induced inhibition of cell division. The presence of some cells showing a short pulse of reporter signal, but no growth inhibition, might hint at stochastic fluctuations in the binding of the repressor LexA or at DNA damage which is so minor that it is repaired before a full-blown SOS response is stimulated.

Studies in *E. coli* have revealed that SOS genes show a heterogeneous expression which is independent of RecA and based on

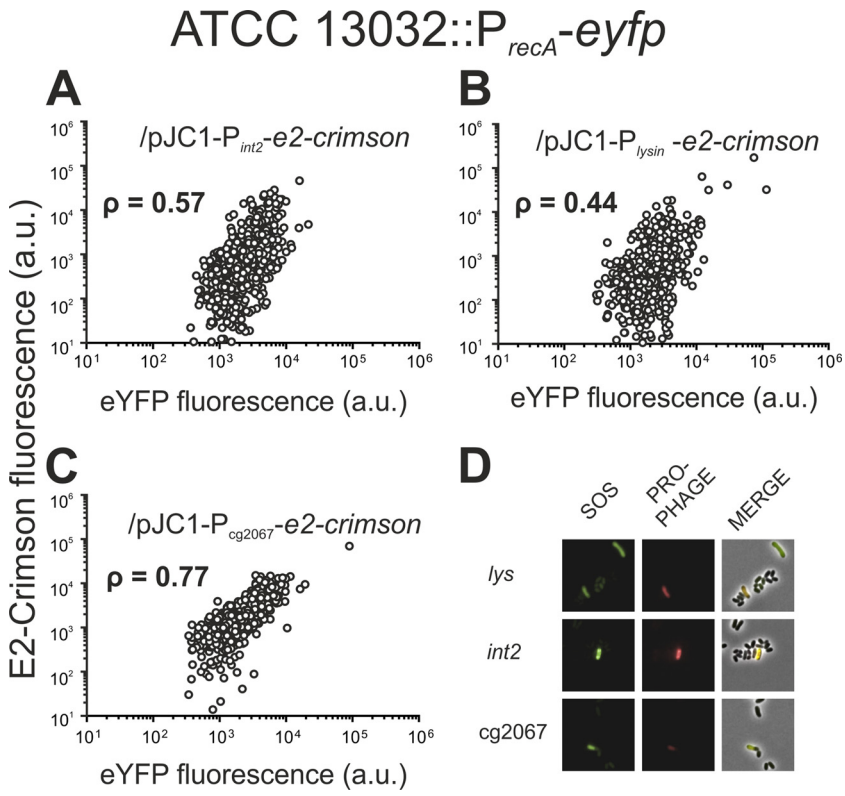

FIG 6 Correlation of P_{recA} reporter activity to the activity of CGP3 genes. Scatter plots of *C. glutamicum* P_{recA}-*eyfp*/pJC1-P_{int2}-*e2-crimson* (A), *C. glutamicum* P_{recA}-*eyfp*/pJC1-P_{lysin}-*e2-crimson* (B), and *C. glutamicum* P_{recA}-*eyfp*/pJC1-P_{cg2067}-*e2-crimson* (C) are shown. Cells with high eYFP fluorescence (SOS^+ cells) were gated and their E2-Crimson fluorescence plotted against their eYFP fluorescence. Spearman's rank correlation coefficient (ρ) was calculated using GraphPad Prism 6. (D) Fluorescence microscopy analysis of cells on agar pads showing the spontaneous induction of SOS and prophage reporters. Cells were cultivated in CGXII medium plus 4% glucose and analyzed at an OD_{600} of 4.

stochastic factors and binding affinities of LexA to SOS boxes (28). To confirm that the spontaneous induction of P_{recA} is caused by a bona fide SOS response, we transformed the P_{recA} reporter strain with plasmids carrying transcriptional fusions of *divS* and *recN* promoters, respectively. The degree of correlation gained by calculating Spearman's ranked correlation coefficient is strong (P_{divS}, $\rho = 0.78$; P_{recN}, $\rho = 0.78$). Whereas this is a strong correlation, higher values of ρ (>0.9) might be expected for causal relationships, as they are present within the SOS cascade. Even though *recA* is upregulated after cells encounter DNA damage, this damage might be repaired before the cell division inhibitor *divS* is induced, thus avoiding a premature inhibition of growth. Our microfluidic experiments showed that this might be the case, as a high number of SOS^+ cells are not inhibited in their growth.

The same applies to the correlation values of the prophage reporters which lie below those observed for the correlation to the SOS reporters. An induced SOS response need not seal the fate of genomic excision for CGP3. Rather, an immunity to low levels of DNA damage and an induction upon accumulation or lasting presence of DNA damage would constitute a more reliable warning system telling the prophage when to "leave the sinking ship." If CGP3 were induced by every event of SOS response, the integration of the prophage would be a rather unstable situation. Thus, a threshold-based model of excision (29), as described for well-studied lambdoid phages, helps to explain the observed deviation from a perfect correlation. Nevertheless, future studies will elucidate the possible influence of so-far unknown regulators that play a role in the induction of CGP3. Microarray studies, for example, revealed that the putative regulator Cg2040 exhibits an inhibitory effect on a set of prophage genes when overexpressed (A. Heyer and J. Frunzke, personal communication).

Finally, we tested our dual promoter fusion strains (P_{recA}-*eyfp*/pJC1-P_{int2}-*e2-crimson*) during a standard flask cultivation experiment to analyze their expression during the course of growth. We observed that P_{recA} and P_{int2} promoters reached their peaks of activation during exponential growth phase. It is reasonable to assume that this phase of rapid cell growth gives rise to intrinsic DNA damage, which is produced by native DNA polymerases. Indeed, it has been reported that replication fork breakage is a major contributor to double-strand breaks (DSBs), which in turn activate the SOS response (30, 31). The measurement of spontaneous activation of the SOS response and prophage activity showed temporally separated peaks (Fig. 7B). As this disparity occurs in a small number of cells, it is clear that this effect would be masked in the bulk measurement of reporter output, as shown in Fig. 7A.

While the consequence of spontaneously inducing prophages has been reported for *Shewanella oneidensis* (7) and *Streptococcus pneumoniae* (8), the effects on *C. glutamicum* on a population-wide scale remain unknown. In studies by Bossi and coworkers (32), a spontaneous induction of prophages led to a competitive fitness of the population against other bacteria. Spontaneous

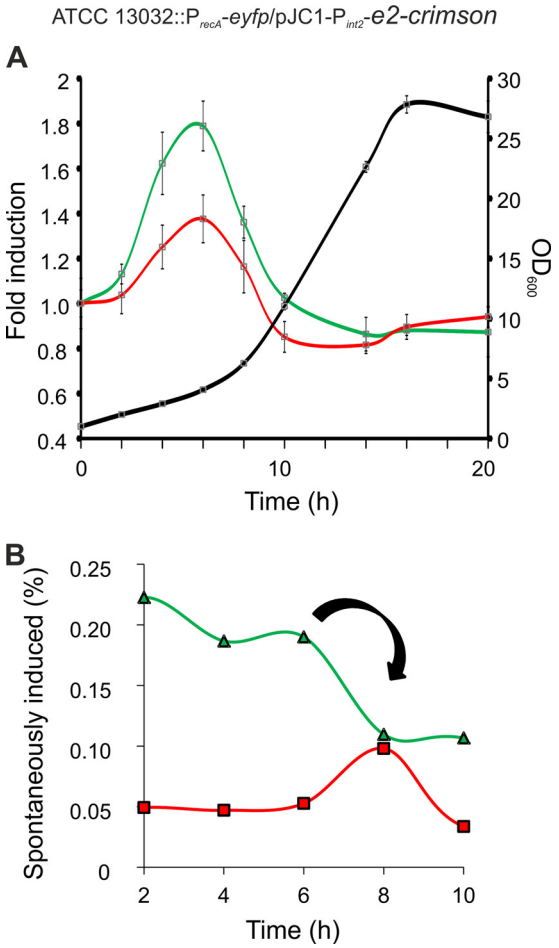

FIG 7 Analysis of activity and spontaneous activation of P_{recA} and P_{int2} during growth. *C. glutamicum* P_{recA}-*eyfp*/pJC1-P_{int2}-*e2-crimson* was cultivated in the Biolector microcultivation system. (A) OD_{600} (black line) and mean eYFP (green line) and E2-Crimson (red line) fluorescence; (B) percentage of cells with a spontaneous P_{recA} (green line) and P_{int2} (red line) induction. The arrow indicates the delay between the peak for maximum spontaneous P_{recA} and maximum spontaneous P_{int2} activity in single cells. Cells were cultivated in CGXII medium plus 4% glucose.

phage release is seen as a strategy to maintain the lysogenic status of the prophage. Immunity sequences within the prophage lead to an immunity to superinfection. Interestingly, the genomic CGP3 locus possesses a restriction-modification system (*cglIM*, *cglIR*, and *cglIIM*) which might be used as a classic toxin/antitoxin module (33) to fend off infecting bacteriophages. An example of "bacterial altruism" was recently described (34) in which Shiga toxin produced by a small number of spontaneously induced prophage works as a positive selective force and benefits the population. The production of toxins by *C. glutamicum* has not been reported, but the release of DNA and proteins into the extracellular matrix as a source of nutrients for the rest of the population or as biofilm matrix for natural microbial communities is a possible scenario. Choosing irreparable or sustained DNA damage as trigger or selection marker to single out "weak individuals" would be a practical approach (35).

Future studies will aim at a more detailed investigation of the phenomenon of spontaneous prophage excision. We have established a first link between the host's SOS response and the excision of the genomically integrated CGP3 prophage in single bacterial cells. Further studies will assess the level at which the two phenomena are linked and which other regulatory pathways may feed into the prophage's decision to excise from the host genome.

ACKNOWLEDGMENTS

For funding we thank the Deutsche Forschungsgemeinschaft (priority program SPP1617) and the Helmholtz Association (Young Investigator grant VH-NG-716).

REFERENCES

1. **Casjens S.** 2003. Prophages and bacterial genomics: what have we learned so far? Mol. Microbiol. **49:**277–300. http://dx.doi.org/10.1046/j.1365–2958.2003.03580.x.
2. **Ajinomoto Co I.** 2011. Food products business. http://www.ajinomoto.com/en/ir/pdf/Feed-useAA-Oct2011.pdf. Ajinomoto Co., Inc., Tokyo, Japan.
3. **Ajinomoto Co I.** 2012. Feed-use amino acids business. http://www.ajinomoto.com/en/ir/pdf/Food-Oct2012.pdf. Ajinomoto Co., Inc., Tokyo, Japan.
4. **Kalinowski J.** 2005. The genomes of amino acid-producing corynebacteria, p 37–56. *In* Eggeling L, Bott M (ed), Handbook of *Corynebacterium glutamicum*. CRC Press, Boca Raton, FL.
5. **Frunzke J, Bramkamp M, Schweitzer J-E, Bott M.** 2008. Population Heterogeneity in *Corynebacterium glutamicum* ATCC 13032 caused by prophage CGP3. J. Bacteriol. **190:**5111–5119. http://dx.doi.org/10.1128/JB.00310-08.
6. **Baumgart M, Unthan S, Rückert C, Sivalingam J, Grünberger A, Kalinowski J, Bott M, Noack S, Frunzke J.** 2013. Construction of a prophage-free variant of *Corynebacterium glutamicum* ATCC 13032—a platform strain for basic research and industrial biotechnology. Appl. Environ. Microbiol. **79:**6006–6015. http://dx.doi.org/10.1128/AEM.01634-13.
7. **Gödeke J, Paul K, Lassak J, Thormann KM.** 2011. Phage-induced lysis enhances biofilm formation in *Shewanella oneidensis* MR-1. ISME J. **5:**613–626. http://dx.doi.org/10.1038/ismej.2010.153.
8. **Carrolo M, Frias MJ, Pinto FR, Melo-Cristino J, Ramirez M.** 2010. Prophage spontaneous activation promotes DNA release enhancing biofilm formation in *Streptococcus pneumoniae*, PLoS One **5:**e15678. http://dx.doi.org/10.1371/journal.pone.0015678.
9. **Flemming H-C, Neu TR, Wozniak DJ.** 2007. The EPS matrix: the "house of biofilm cells." J. Bacteriol. **189:**7945–7947. http://dx.doi.org/10.1128/JB.00858-07.
10. **Whitchurch CB, Tolker-Nielsen T, Ragas PC, Mattick JS.** 2002. Extracellular DNA required for bacterial biofilm formation. Science **295:**1487. http://dx.doi.org/10.1126/science.295.5559.1487.
11. **Lwoff A.** 1953. Lysogeny. Bacteriol. Rev. **17:**269–332.
12. **Luria.** 1967. Transduction studies on the role of a rec$^+$ gene in the ultraviolet induction of prophage lambda. J. Mol. Biol. **23:**117–133. http://dx.doi.org/10.1016/S0022-2836(67)80021-4.
13. **Oppenheim AB, Kobiler O, Stavans J, Court DL, Adhya S.** 2005. Switches in bacteriophage lambda development. Annu. Rev. Genet. **39:**409–429. http://dx.doi.org/10.1146/annurev.genet.39.073003.113656.
14. **Friedberg EC, Walker GC, Siede W, Wood RD, Schultz RA, Ellenberger T.** 2005. DNA repair and mutagenesis. ASM Press, Washington, DC.
15. **Grünberger A, Paczia N, Probst C, Schendzielorz G, Eggeling L, Noack S, Wiechert W, Kohlheyer D.** 2012. A disposable picolitre bioreactor for cultivation and investigation of industrially relevant bacteria on the single cell level. Lab. Chip. **12:**2060–2068. http://dx.doi.org/10.1039/c2lc40156h.
16. **Mustafi N, Grünberger A, Kohlheyer D, Bott M, Frunzke J.** 2012. The development and application of a single-cell biosensor for the detection of L-methionine and branched-chain amino acids. Metab. Eng. **14:**449–457. http://dx.doi.org/10.1016/j.ymben.2012.02.002.
17. **Keilhauer C, Eggeling L, Sahm H.** 1993. Isoleucine synthesis in *Corynebacterium glutamicum*: molecular analysis of the *ilvB-ilvN-ilvC* operon. J. Bacteriol. **175:**5595–5603.
18. **Kensy F, Zang E, Faulhammer C, Tan R-K, Büchs J.** 2009. Validation of a high-throughput fermentation system based on online monitoring of biomass and fluorescence in continuously shaken microtiter plates. Microb. Cell Fact. **8:**31. http://dx.doi.org/10.1186/1475-2859-8-31.

19. **Inoue H, Nojima H, Okayama H.** 1990. High efficiency transformation of *Escherichia coli* with plasmids. Gene **96:**23–28. http://dx.doi.org/10.1016/0378-1119(90)90336-P.
20. **Van der Rest ME, Lange C, Molenaar D.** 1999. A heat shock following electroporation induces highly efficient transformation of *Corynebacterium glutamicum* with xenogeneic plasmid DNA. Appl. Microbiol. Biotechnol. **52:**541–545. http://dx.doi.org/10.1007/s002530051557.
21. **Eikmanns B, Thum-Schmitz N.** 1994. Nucleotide sequence, expression and transcriptional analysis of the *Corynebacterium glutamicum gltA* gene encoding citrate synthase. Microbiology **140:**1817–1828. http://dx.doi.org/10.1099/13500872-140-8-1817.
22. **Jochmann N, Kurze AK, Czaja LF, Brinkrolf K, Brune I, Hüser AT, Hansmeier N, Pühler A, Borovok I, Tauch A.** 2009. Genetic makeup of the *Corynebacterium glutamicum* LexA regulon deduced from comparative transcriptomics and in vitro DNA band shift assays. Microbiology **155:**1459–1477. http://dx.doi.org/10.1099/mic.0.025841-0.
23. **Hentschel E, Will C, Mustafi N, Burkovski A, Rehm N, Frunzke J.** 2013. Destabilized eYFP variants for dynamic gene expression studies in *Corynebacterium glutamicum*, Microb. Biotechnol. **6:**196–201. http://dx.doi.org/10.1111/j.1751-7915.2012.00360.x.
24. **Strack RL, Hein B, Bhattacharyya D, Hell SW, Keenan RJ, Glick BS.** 2009. A rapidly maturing far-red derivative of DsRed-Express2 for whole-cell labeling. Biochemistry **48:**8279–8281. http://dx.doi.org/10.1021/bi900870u.
25. **Grünberger A, Probst C, Heyer A, Wiechert W, Frunzke J, Kohlheyer D.** Microfluidic picoliter bioreactor for microbial single cell analysis: fabrication, system setup and operation. J. Vis Exp., in press.
26. **Ogino H, Teramoto H, Inui M, Yukawa H.** 2008. DivS, a novel SOS-inducible cell-division suppressor in *Corynebacterium glutamicum*, Mol. Microbiol. **67:**597–608. http://dx.doi.org/10.1111/j.1365-2958.2007.06069.x.
27. **Pennington JM, Rosenberg SM.** 2007. Spontaneous DNA breakage in single living *Escherichia coli* cells. Nat. Genet. **39:**797–802. http://dx.doi.org/10.1038/ng2051.
28. **Kamenšek S, Podlesek Z, Gillor O, Zgur-Bertok D.** 2010. Genes regulated by the *Escherichia coli* SOS repressor LexA exhibit heterogeneous expression. BMC Microbiol. **10:**283. http://dx.doi.org/10.1186/1471-2180-10-283.
29. **Bailone A, Levine A, Devoret R.** 1979. Inactivation of prophage λ repressor in vivo. J. Mol. Biol. **131:**553–572. http://dx.doi.org/10.1016/0022-2836(79)90007-X.
30. **Cox MM, Goodman MF, Kreuzer KN, Sherratt DJ, Sandlerk SJ, Marians KJ.** 2000. The importance of repairing stalled replication forks. Nature **2:**37–41.
31. **Rothstein R, Michel B, Gangloff S.** 2000. Replication fork pausing and recombination or "gimme a break." Gene Dev. **14:**1–10.
32. **Bossi L, Fuentes J, Mora G, Figueroa-Bossi N.** 2003. Prophage contribution to bacterial population dynamics. J. Bacteriol. **185:**6467–6471. http://dx.doi.org/10.1128/JB.185.21.6467-6471.2003.
33. **Makarova KS, Wolf YI, Koonin EV.** 2009. Comprehensive comparative-genomic analysis of type 2 toxin-antitoxin systems and related mobile stress response systems in prokaryotes. Biol. Direct **4:**19. http://dx.doi.org/10.1186/1745-6150-4-19.
34. **Loœ JM, Loœ M, Wêgrzyn A, Wêgrzyn G.** 2012. Altruism of Shiga toxin-producing *Escherichia coli*: recent hypothesis versus experimental results. Front. Cell Infect. Microbiol. **2:**166. http://dx.doi.org/10.3389/fcimb.2012.00166.
35. **Watve M, Parab S, Jogdand P, Keni S.** 2006. Aging may be a conditional strategic choice and not an inevitable outcome for bacteria. Proc. Natl. Acad. Sci. U. S. A. **103:**14831–14835. http://dx.doi.org/10.1073/pnas.0606499103.
36. **Kinoshita S, Udaka S, Shimono M.** 2004. Studies on the amino acid fermentation. Part 1. Production of L-glutamic acid by various microorganisms. J. Gen. Appl. Microbiol. **50:**331–343. http://dx.doi.org/10.2323/jgam.3.193.
37. **Schäfer A, Tauch A, Jäger Kalinowski WJ, Thierbach G, Pühler A.** 1994. Small mobilizable multi-purpose cloning vectors derived from the Escherichia coli plasmids pK18 and pK19: selection of defined deletions in the chromosome of *Corynebacterium glutamicum*, Gene **145:**69–73. http://dx.doi.org/10.1016/0378-1119(94)90324-7.
38. **Cremer J, Eggeling L, Sahm H.** 1991. Control of the lysine biosynthesis sequence in Corynebacterium glutamicum as analyzed by overexpression of the individual corresponding genes. Appl. Environ. Microbiol. **57:**1746–1752.